

Electrochemical Hydrogen Generation by Biomass Electrolysis with Pt₂MoS₂ Electrode

Maria Sarno^{a,b*}, Eleonora Ponticorvo^b

^a Department of Physics "E.R. Caianiello", University of Salerno, Via Giovanni Paolo II, 132, 84084, Fisciano (SA), Italy.

^b NanoMates, Research Centre for Nanomaterials and Nanotechnology at the University of Salerno, University of Salerno, Via Giovanni Paolo II, 132, 84084, Fisciano (SA), Italy.

msarno@unisa.it

Here we report the performance in lignocellulosic material oxidation of Pt₂MoS₂-based electrode. The prepared nanocomposite, synthesized according to a "wet chemistry" approach, was broadly characterized: SEM-EDS images and XRD spectrum indicate the formation of nanoparticles with a few nanometers size dispersed on MoS₂ nanosheets. The sample was tested for the oxidation of lignocellulosic biomass in alkaline solutions. A very small overpotential is demonstrated (0.17 V) showing that such process could significantly reduce the cost of generating hydrogen reducing the energy required for the anodic oxidation process.

1. Introduction

In recent years, hydrogen has been regarded as the best alternative to fossil fuels (Dincer and Acar, 2015; Cortright et al., 2002). Steam reforming is typically adopted for large scale H₂ production (Heinzel et al., 2002). On the other hand, it requires temperatures higher than 600 °C and produces low purity hydrogen with a high concentration of CO and CO₂. Therefore, additional separation units are needed to obtain pure H₂. With water electrolysis, it's possible to achieve large pure hydrogen production starting from readily accessible, cheap and renewable resources. In particular, in the case of abundant renewable energy availability, the excess of energy can be stored in the form of H₂ via water electrolysis (Zeng and Zhang, 2010).

The main water electrolysis disadvantage is the high electrical energy requirements; the electrolysis of organic molecules is a promising alternative for H₂ generation since the minimum thermodynamic potential needed for the electro-oxidation of the organic molecules is about one order of magnitude lower than that for water electrolysis. Pure H₂ can be produced by the electrolysis of methanol (Sapountzi et al., 2017; Sarno et al., 2019), ethanol (Gutiérrez-Guerra et al., 2015) and bioethanol (Caravaca et al., 2013) solutions. However, some alcohols are already considered as important bio-fuels. Therefore, their further transformation to H₂ is unattractive for practical purposes. Lignin is one of the most available bio-polymers in nature (Mohana Roopan, 2017), its abundant amount as a natural product or by-product from different processes, has led to its utilization as feedstock for chemicals compounds and biofuels production. Numerous approaches have been developed for lignin degradation: thermochemical, catalytic and enzymatic processes have been studied (Pandey and Kim, 2011); however, challenges still persist for the development of processes with high efficiency and low cost.

Electrochemistry allows working under moderate conditions compared to conventional processes. To enhance the potential of biomass-derived molecules (such as lignocellulosic materials) as an H₂ resource, this technology should be improved. Platinum is the best catalyst in numerous electrochemical processes, considering the high cost and the low abundance of Pt there is a significant need to develop new active and cheap electrocatalysts. Molybdenum disulfide (MoS₂) (Li et al., 2018) has attracted great attention because of its high ability for accepting electrons and protons. This material exhibits excellent corrosion resistance compared to other transition metal composites and similar electronic properties of Pt-group metals. In this study, we present hydrogen production by the direct electrochemical oxidation of a lignocellulosic biomass. The combined use of different techniques was used to characterize the synthesized nanomaterial. The hydrogen yield per weight of biomass was determined in a batch electrochemical cell. Scanning Electron

Microscopy, Energy-dispersive X-ray spectroscopy, X-ray diffraction, and thermogravimetric analysis were employed for nanomaterials characterization.

2. Experimental Section

2.1 Nanocomposite synthesis

Platinum (III) acetylacetonate (0.5 mmol) and ammonium tetrathiomolybdate (2 mmol) were loaded into the reagent mixture, consisting of 20 ml of 1-octadecene, oleic acid (6 mmol), oleylamine (6 mmol) and 1,2-hexadecandiol (10 mmol) as reducing agent. The temperature was increased to 200°C for 2 h and then the mixture was heated up to 285°C for 1 h, in an inert ambient (Sarno et al., 2018; Sarno et al., 2016). After synthesis, Pt/MoS₂ nanocomposite obtained was purified alternating ethanol and hexane washing and separating by centrifugation (Sarno and Ponticorvo, 2019). To remove the organic content, thermal treatment at 150 °C for 8h followed.

2.2 Characterization methods

Scanning electron microscopy (SEM) was performed through the use of a LEO 1525 electron microscope and an energy dispersive X-ray (EDX) probe. Thermogravimetric analysis (TG-DTG) was carried out by using an SDTQ 600 Analyzer (TA Instruments) with a heating rate of 10 °C/min, from ambient temperature up to 1000 °C under airflow (Ciambelli et al., 2004; Sarno et al., 2012). Electrochemical characterization was carried out by means of Autolab PGSTAT302N potentiostat/galvanostat. To obtain the electrodes, 4 mg of synthesized nanocomposites were dispersed into 80 µl of a 5 wt% Nafion solution, 200 µl of ethanol and 800 µl of distilled water. The solution was partly deposited dropwise onto a Screen Printed Electrode (SPE) consisting of a Pt working electrode, a Pt counter electrode and a Ag reference electrode. Biomass (wood sawdust, particles size >10 µm 13.5 %, 2.6-10 µm 19.2 %, 0.1-2.6 µm 24.1 %, <0.1 µm 43.2 %) electrochemical conversion was evaluated in 1 M NaOH solution with a biomass concentration of 10 g/L. The electrocatalyst performance was evaluated also in the absence of biomass. Nitrogen was supplied continuously to the cell. The working electrode potential was then held constant for three hours, after which the solution was collected and analyzed via FT-IR (Vertex 70 apparatus (Bruker Corporation) by applying KBr technique) and UV-vis spectroscopy (Thermo-Scientific UV-vis Evolution Q60 spectrophotometer) to evaluate the modification of the biomass structure via electrochemical oxidation.

3. Results and discussion

3.1 Nanocomposite characterization

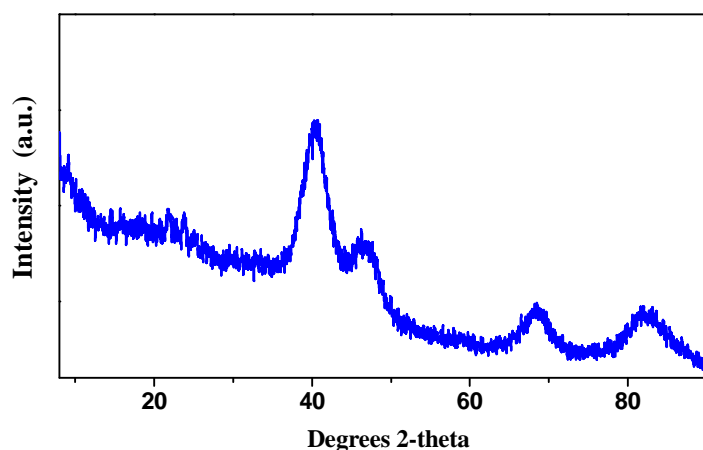


Figure 1: XRD spectrum of Pt/MoS₂ NPs

In Figure 1 The X-ray diffraction pattern of Pt/MoS₂ nanocomposite is shown. In particular, the typical peaks of platinum are visible, i.e. peaks at 39.2° (111), 45.1° (200), 67.3° (220), 82.1° (311) can be detected. The Pt crystalline size measured by Scherrer's equation was found to be 2.5 ± 0.3 nm (Sarno et al., 2014). Furthermore, a very weak MoS₂ nanosheets peak was observed at 58.9°, corresponding to (110) plane (Sarno

and Ponticorvo, 2017). The absence of (002) plane and the broadness of peak indicate that the obtained MoS_2 is a single layer or few-layer graphene-like MoS_2 .

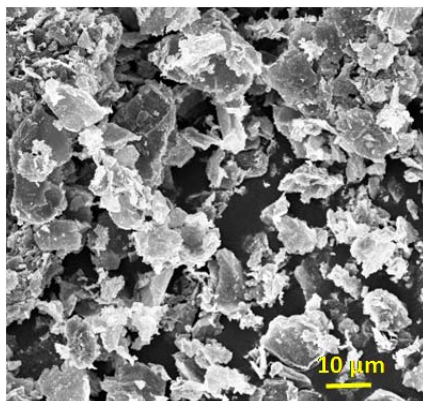


Figure 2: SEM image of Pt_MoS_2 NPs

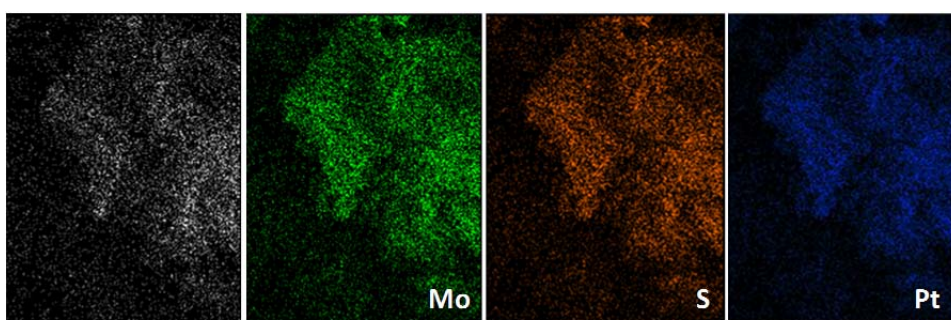


Figure 3: EDS maps of Pt_MoS_2 NPs

SEM measurements (Figure 2) were performed to evaluate the layers' size of MoS_2 . The nanocomposite resulted constituted of layers varying from few micrometers to about twenty micrometers. Energy-dispersive X-ray spectroscopy (EDS) mapping with distributions of Mo, S, and Pt are shown in Figure 3. In this EDS mapping, Pt is found in the entire area indicating that Pt NPs are present everywhere within the observed window, as expected. Moreover, Mo and S are distributed in a similar manner in the sample.

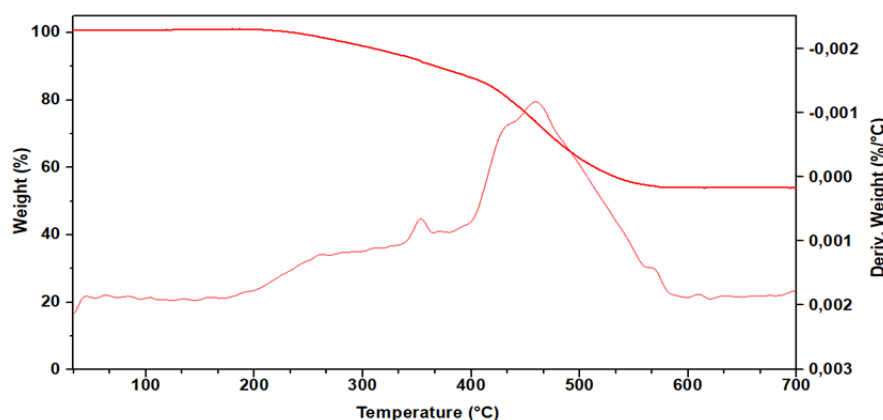


Figure 4: TG-DTG profile of Pt_MoS_2 NPs

The prepared electrode was characterized by the help of thermogravimetric analysis. During the thermal conversion of Pt_MoS_2 in airflow, a decomposition-oxidation of the oleylamine/oleic acid organic chains covering the nanocomposite happens together with an SO_2 release. After the sulfur/impurities oxidation, in the

temperature range 207–400 °C, at ~400 °C the oxidation of MoS₂ to MoO₃ with SO₂ release starts. At 700 °C, a residue of 54% was observed, which is due to Pt and residual, non-sublimated, MoO₃.

3.2 Lignocellulosic biomass electrolysis

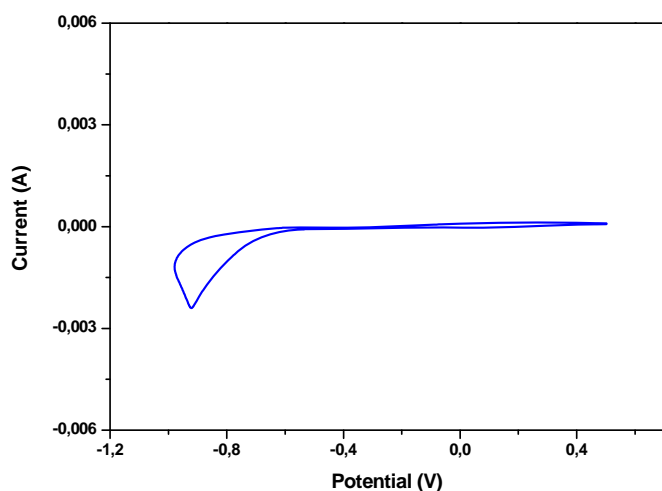


Figure 5: Cyclic voltammetry on Pt_MoS₂ electrode in 1 M NaOH at 20 mV/s of scan rate.

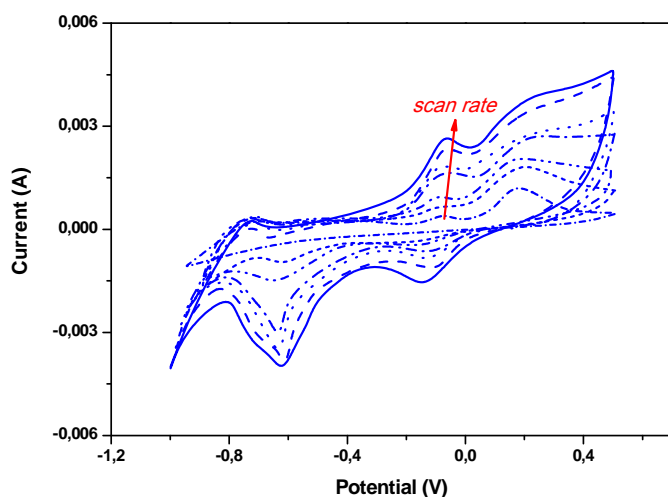


Figure 6: Cyclic voltammetry on Pt_MoS₂ electrode in 1 M NaOH and 10 g/L of lignocellulosic material at increasing scan rate (20-500 mV/s).

The prepared electrode was firstly characterized by cyclic voltammetry (CV) in 1 M NaOH solution in the absence of biomass (Figure 5). During the CV test no evident oxidation peaks are visible (i.e. no electrode oxidation/passivation), on the other hand, hydrogen evolution reaction (HER) occurs at the low overpotential of 0.56 V, it should be noted that the voltage was not adjusted according to the standard hydrogen electrode, thus the corrected overpotential is below to 0.2 V.

In Figure 6 CV measurements with a biomass concentration of 10 g/L, at increasing scan rates, are shown. Oxidation peaks are clearly visible, attributed to electrochemical oxidation of biomass or its oxidation products or active intermediates, mediated by •OH radicals leading to removal of an electron from the biopolymers or its active intermediates (Wang et al., 2015). Figure 6 show also increments of the anodic and cathodic peaks at increased scan rates, shifts in the anodic direction of the oxidation peaks and shifts in the cathodic direction of the reduction peaks upon increasing scan rate can be also noted, suggesting that the reactions of biomass on the Pt_MoS₂ electrode are irreversible (Sarno and Ponticorvo, 2019; Gowda and Nandibewoor, 2014).

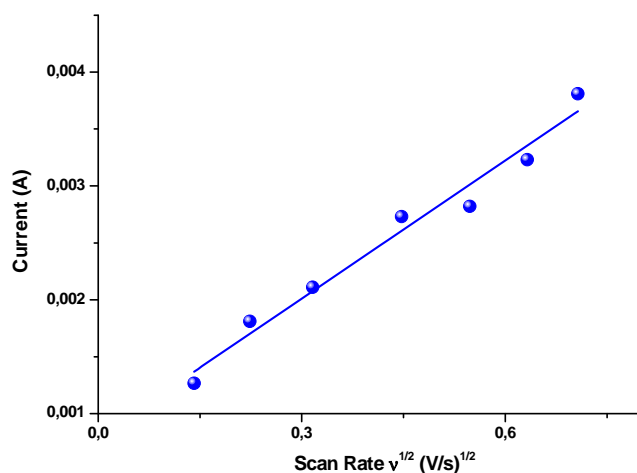


Figure 7: Variation of oxidation peak vs. scan rate.

Diffusion control of charge transfer processes involving biomass is demonstrated by observing the behavior of the anodic peak as a function of scan rate, as shown in Figure 7.

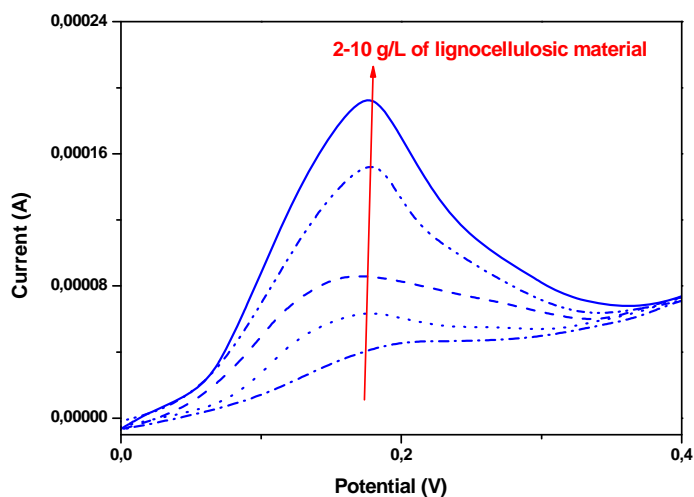


Figure 8: Linear sweep voltammograms on Pt_MoS_2 electrode in 1 M NaOH solution at increasing concentrations of lignocellulosic material (concentration range: 2-10 g/L), scan rate: 20 mV/s.

The electrochemical behavior of the Pt_MoS_2 electrode was also studied under biomass concentration increases: linear sweep voltammograms (LSVs) recorded at the concentrations range 2-10 g/L are shown in Figure 8. The oxidation peak at ~ 0.2 V is observed, which becomes more defined and with higher peak currents as the biomass concentration increases, showing that this process is biomass concentration dependent, and that higher biomass concentrations, close to the electrode surface, can increase the rate of reaction, which is a characteristic behavior of several electrochemical processes.

4. Conclusions

In summary, a simple and efficient strategy was applied to synthesize a Pt_MoS_2 based electrode. XRD, SEM, EDS and TG-DTG analysis confirmed the formation of the aforementioned nanocomposite structure. The prepared nanocomposite has been tested as electrochemical catalyst in order to oxidize lignocellulosic biomass in aqueous solutions, to give pure H_2 at the cathode, at lower potentials than required for oxygen evolution (~ 0.8 V in alkaline media). Our results indicate that lignin oxidation is irreversible, forming oxidation products that likely further react via homogenous chemical reactions or additional heterogeneous charge transfer steps.

Importantly, no oxidation/reduction processes of the electrocatalyst occurred during biomass oxidation process.

Further studies will be focused on the collection and quantification of the hydrogen production rate at the counter electrode.

References

- Caravaca A., De Lucas-Consuegra A., Calcerrada A.B., Lobato J., Valverde J.L., Dorado F., 2013, From biomass to pure hydrogen: electrochemical reforming of bioethanol in a PEM electrolyser, *Applied Catalysis B: Environmental*, 134–135, 302–309.
- Ciambelli P., Sannino D., Sarno M., Fonseca A., Nagy J.B., 2004, Hydrocarbon decomposition in alumina membrane: An effective way to produce carbon nanotubes bundles, *Journal of Nanoscience and Nanotechnology*, 4, 779–787.
- Cortright R.D., Davda R.R., Dumesic J.A., 2002, Hydrogen from catalytic reforming of biomass-derived hydrocarbons in liquid water, *Nature*, 418, 964–967.
- Dincer I., Acar C., 2015, Review and evaluation of hydrogen production methods for better sustainability, *International Journal of Hydrogen Energy*, 40, 11094–11111.
- Gowda J.I., Nandibewoor S.T., 2014, Electrochemical behavior of paclitaxel and its determination at glassy carbon electrode, *Asian Journal of Pharmaceutical Sciences*, 9, 42–49.
- Gutiérrez-Guerra N., Jiménez-Vázquez M., Serrano-Ruiz J.C., Valverde J.L., de Lucas-Consuegra A., 2015, Electrochemical reforming vs. catalytic reforming of ethanol: a process energy analysis for hydrogen production, *Chemical Engineering and Processing: Process Intensification*, 95, 9–16.
- Heinzel A., Vogel B., Hübner P., 2002, Reforming of natural gas - hydrogen generation for small scale stationary fuel cell systems, *Journal of Power Sources*, 105, 202–207.
- Li D., Li Y., Zhang B., Lui Y.H., Mooni S., Chen R., Hu S., Ni H., 2018, Insertion of Platinum Nanoparticles into MoS₂ Nanoflakes for Enhanced Hydrogen Evolution Reaction, *Materials*, 11, 1520.
- Mohana Roopan S., 2017, An overview of natural renewable bio-polymer lignin towards nano and biotechnological applications, *International Journal of Biological Macromolecules*, 103, 508–514.
- Pandey M. P., Kim C. S., 2011, Lignin Depolymerization and Conversion: A Review of Thermochemical Methods, 34, 29–41.
- Sapountzi F.M., Tsampas M.N., Fredriksson H.O.A., Gracia J.M., Niemantsverdriet J.W., 2017, Hydrogen from electrochemical reforming of C1–C3 alcohols using proton conducting membranes, *International Journal of Hydrogen Energy*, 42, 10762–10774.
- Sarno M., Cirillo C., Ciambelli P., 2014, Selective graphene covering of monodispersed magnetic nanoparticles, *Chemical Engineering Journal*, 246, 27–38.
- Sarno M., Cirillo C., Scudieri C., Polichetti M., Ciambelli P., 2016, Electrochemical Applications of Magnetic Core–Shell Graphene-Coated FeCo Nanoparticles, *Industrial and Engineering Chemistry Research*, 55, 3157–3166.
- Sarno M., Ponticorvo E., 2018, MoS₂/ZnO nanoparticles for H₂S removal, *Chemical Engineering Transactions* 68, 481–486.
- Sarno M., Ponticorvo E., 2019, Metal–metal oxide nanostructure supported on graphene oxide as a multifunctional electro-catalyst for simultaneous detection of hydrazine and hydroxylamine, *Electrochemistry Communications*, 107, 106510.
- Sarno M., Ponticorvo E., Scarpa D., 2019, PtRh and PtRh/MoS₂ nano-electrocatalysts for methanol oxidation and hydrogen evolution reactions, *Chemical Engineering Journal*, 377, 120600.
- Sarno M., Sannino D., Leone C., Ciambelli P., 2012, Evaluating the effects of operating conditions on the quantity, quality and catalyzed growth mechanisms of CNTs, *Journal of Molecular Catalysis A: Chemical*, 357, 26–38.
- Sarno M., Ponticorvo E., 2017, Effect of the amount of nickel sulphide, molybdenum disulphide and carbon nanosupport on a Tafel slope and overpotential optimization, *Nanotechnology*, 28, 214003.
- Wang Y.-s., Yang F., Liu Z.-h, Yuan L., Li G., 2015, Electrocatalytic degradation of aspen lignin over Pb/PbO₂ electrode in alkaline solution, *Catalysis Communications*, 67, 49–53.
- Zeng K., Zhang D., 2010, Recent progress in alkaline water electrolysis for hydrogen production and applications, *Progress in Energy and Combustion Science*, 36, 307–326.